Journal of Sound and Vibration 329 (2010) 1390–1408

Contents lists available at ScienceDirect

Journal of Sound and Vibration

journal homepage: www.elsevier.com/locate/jsvi

Closed-form solution for free vibration of piezoelectric coupled annular plates using Levinson plate theory

Sh. Hosseini Hashemi, M. Es'haghi, M. Karimi *

Impact Research Laboratory, School of Mechanical Engineering,, Iran University of Science and Technology, Narmak, Tehran 16848-13114, Iran

A R T I C L E I N F O

Article history:
Received 2 July 2009
Received in revised form
13 October 2009
Accepted 14 October 2009
Handling Editor: A.V. Metrikine
Available online 16 December 2009

A B S T R A C T

Free vibration analysis of annular moderately thick plates integrated with piezoelectric layers is investigated in this study for different combinations of soft simply supported, hard simply supported and clamped boundary conditions at the inner and outer edges of the annular plate on the basis of the Levinson plate theory (LPT). The distribution of electric potential along the thickness direction in the piezoelectric layer is assumed as a sinusoidal function so that the Maxwell static electricity equation is approximately satisfied. The differential equations of motion are solved analytically for various boundary conditions of the plate. In this study the closed-form solution for characteristic equations, displacement components of the plate and electric potential are derived for the first time in the literature. To demonstrate the accuracy of the present solution, comparison studies is first carried out with the available data in the literature and then natural frequencies of the piezoelectric coupled annular plate are presented for different thickness-radius ratios, inner–outer radius ratios, thickness of piezoelectric, material of piezoelectric and boundary conditions. Present analytical model provides design reference for piezoelectric material application, such as sensors, actuators and ultrasonic motors.

1. Introduction

Annular plates are often found in the construction of various structural systems, including civil, mechanical, space structures, electronic components, marine structures and nuclear engineering. A good understanding of the dynamic behaviors for these structural components is crucial to the design and performance evaluation of mechanical systems. A vast amount of literature for free vibration studies of circular and annular plates is available. Many studies on this subject have been experimentally and theoretically carried out by many researchers such as Leissa [1], Irie et al. [2], So and Leissa [3], Liew and Yang [4], Efraim and Eisenberger [5], Liu and Lee [6] and Zhou et al. [7].

The classical plate theory (CPT) furnishes accurate and reliable solutions for most thin plate analysis. When plate thickness increases, CPT over predicts vibration response because transverse shear deformation and rotary inertia effects are neglected. As a natural extension, first-order theory and higher-order theory were developed to incorporate the shear deformation effect. These theories can be applied to moderately thick plate analysis to overcome the drawback of CPT. Using of higher-order plate theories generally leads to a more accurate prediction of the global response quantities such as deflections, buckling loads, and natural frequencies especially in thick plates.

* Corresponding author. Tel.: +98 2177 240 190; fax: +98 2177 24 0488.
E-mail addresses: mkarimi@mecheng.iust.ac.ir, karimi.mahmoud@mapnaturbine.com (M. Karimi).

0022-460X/$ - see front matter
doi:10.1016/j.jsv.2009.10.043

The first-order shear deformation plate theory was proposed by Reissner [8], and developed further for the deformable plates in statics and dynamics by Mindlin et al. [9,10]. In the Mindlin theory, the constant shear stress condition violates the statical condition of zero shear stress at the free surfaces. To compensate for the error, Mindlin introduces shear correction factors to modify the shear forces. A more sophisticated plate theory proposed by Reddy [11] assumes the normal to bend in a form of a cubic curve that ensures the satisfaction of zero shear strain at the free surfaces of the plate. Levinson [12] presented an accurate simple theory for the static and dynamic analysis of rectangular plates. He used a vector approach to derive his equations of equilibrium of homogeneous plates. Levinson plate theory serves as a compromise between the Mindlin plate theory and the Reddy plate theory. The theory captures the higher-order effect by assuming the same third-order polynomials in the expansion of the in-plane displacement components as in the Reddy plate theory and therefore it avoids the need of a shear correction factor. Moreover, its total order of governing equation remains at the fourth order level that is similar to both the Mindlin and the classical thin plate theories whereas the total order of governing equation of the Reddy plate theory is six. The Levinson theory has these features because it neglects the higher-order moments and higher-order shear forces that appear in the variational formulation of the Reddy plate theory. Wang and Kitipornchai [13] presented an exact frequency relationship between Levinson plate theory and Kirchhoff plate theory for homogeneous plates of general polygonal shape and simply supported edges. Reddy et al. [14] derived the exact relationships between the bending solutions of the Levinson and Kirchhoff beam and plate theories based on the load equivalence and mathematical similarity of the governing equations of the both mentioned theories. A comprehensive work on edge-zone equation of linear and non-linear shear deformation theories of symmetric laminated plates was done by Nosier and Reddy [15,16].

Due to the widespread use of the piezoelectric materials in sensors and actuators, the study of embedded or surface-mounted piezoelectric materials has received considerable attention in recent years. Tiersten [17] formulated the governing equations for the vibration of piezoelectric plates and investigated their fundamental electro-mechanical behavior. The general solutions for the dynamic equations of a transversely isotropic piezoelectric medium were investigated by Ding et al. [18]. Wang et al. [19] and Liu et al. [20] analyzed the free vibration of a piezoelectric coupled thin and thick circular plate. Their hypotheses that the distribution of electric potential along the thickness direction in the piezoelectric layer is simulated by a sinusoidal function were validated by FE analysis and analytical solutions satisfying Maxwell static electricity equation were presented. Duan et al. [21] used the Mindlin plate theory (MPT) to investigate the free vibration analysis of piezoelectric coupled thin and thick annular plate. Liu et al. [22] reported a modified axisymmetric finite element for the 3-D vibration analysis of piezoelectric laminated circular and annular plates. Zhang and Sun [23] conducted a study on the analysis of a sandwich plate structure containing a piezoelectric core, where an electric field in the thickness direction may generate shear deformation within the core.

To distinguish the present work from those available in the literature, the main objective of this paper is to present a closed-form solution for the free vibration analysis of piezoelectric coupled moderately thick annular plates with different combinations of soft simply supported, hard simply supported and clamped boundary conditions at the inner and outer edges by using the Levinson plate theory. The solutions can also serve as benchmarks for validations of numerical techniques. First, results obtained by the present solution are compared with existing numerical data. Second, the effect of plate parameters such as thickness-radius ratios, inner–outer radius ratios, as well as boundary conditions and piezoelectric parameters such as thickness of piezoelectric and material of piezoelectric on natural frequencies of the plate is comprehensively investigated. Finally, some 3-D mode shapes of the annular Levinson plates coupled with Piezoelectric are illustrated.

2. Constitutive relations for a piezoelectric sandwich plate based on LPT

2.1. Displacement field

Consider a thick laminated annular plate consisting of one host layer and two piezoelectric layers with outer radius r_0, inner radius r_1, host layer thickness $2h$ and piezoelectric layer thickness h_p. Both top and bottom surfaces of each piezoelectric layer are fully covered by electrodes that are shortly connected. As depicted in Fig. 1 both piezoelectric layers are polarized perpendicular to the mid-plane in the positive direction of the z-axis. The plate geometry and dimensions are defined in an orthogonal cylindrical coordinate system (r,θ,z). In the Levinson plate theory, the displacement components are assumed to be given by

$$u(r,\theta,z,t)=u_0(r,\theta,t)+z\psi_r(r,\theta,t)-\frac{1}{3(h+h_p)^2}z^3\left(\psi_r(r,\theta,t)+\frac{\partial w(r,\theta,t)}{\partial r}\right),$$

$$v(r,\theta,z,t)=v_0(r,\theta,t)+z\psi_\theta(r,\theta,t)-\frac{1}{3(h+h_p)^2}z^3\left(\psi_\theta(r,\theta,t)+\frac{\partial w(r,\theta,t)}{r\partial\theta}\right),$$

$$w(r,\theta,t)=w_0(r,\theta,t), \tag{1a−c}$$

where w, u, and v are the displacements in the transverse, radial and tangential direction of the plate, respectively; u_0 and v_0 denote the in-plane displacements on mid-plane and w_0 is transverse displacement on mid-plane; ψ_r and ψ_θ are the

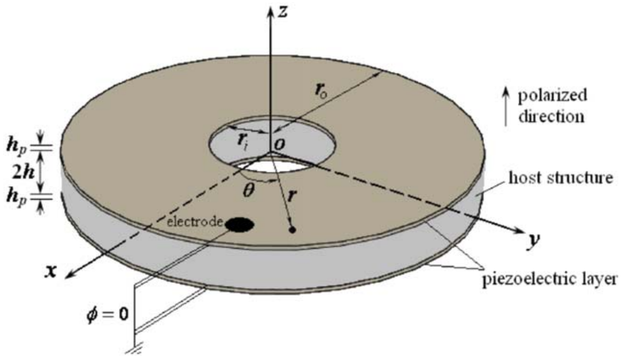

Fig. 1. Sketch of an annular plate surface mounted with two piezoelectric layers.

slope rotations in the $r-z$ and $\theta-z$ planes at $z=0$, respectively, and t is the time. In this study, since the flexural vibration of the plate can only be studied, the in-plane displacements u_0 and v_0 are omitted. For simplicity, the notation w is used for w_0 in the following derivation of the governing equations of plate.

2.2. Strain and stress field in sandwich plate

The strain components of the host plate and piezoelectric layer are given by

$$\varepsilon_r = \frac{\partial u}{\partial r}, \quad \varepsilon_\theta = \frac{u}{r} + \frac{\partial v}{r\partial \theta}, \quad \varepsilon_z = 0, \tag{2a–c}$$

$$\varepsilon_{r\theta} = \frac{\partial v}{\partial r} + \frac{\partial u}{r\partial \theta} - \frac{v}{r}, \quad \varepsilon_{rz} = \frac{\partial u}{\partial z} + \frac{\partial w}{\partial r}, \quad \varepsilon_{\theta z} = \frac{\partial v}{\partial z} + \frac{\partial w}{r\partial \theta}, \tag{2d–f}$$

where $\partial(\bullet)/\partial r$ ($\bullet = u, v$ and w), for example, denotes the partial derivative with respect to r; ε_r and ε_θ are the normal strains and $\varepsilon_{r\theta}$, ε_{rz} and $\varepsilon_{\theta z}$ are the shear strains.

The stress components in the host plate are expressed as

$$\sigma_r^h = \frac{E}{1-\nu^2}(\varepsilon_r + \nu\varepsilon_\theta),$$

$$\sigma_\theta^h = \frac{E}{1-\nu^2}(\varepsilon_\theta + \nu\varepsilon_r),$$

$$\tau_{r\theta}^h = \frac{E}{2(1+\nu)}\varepsilon_{r\theta},$$

$$\tau_{rz}^h = \frac{E}{2(1+\nu)}\varepsilon_{rz},$$

$$\tau_{\theta z}^h = \frac{E}{2(1+\nu)}\varepsilon_{\theta z}, \tag{3a–e}$$

where the superscript h represents the variables in the host structure, E and ν are the Young's modulus and Poisson ratio of the host material, respectively. The constitutive relations in the piezoelectric layer are written as

$$\sigma_r^E = \overline{C}_{11}^E \varepsilon_r + \overline{C}_{12}^E \varepsilon_\theta - \overline{e}_{31} E_z,$$

$$\sigma_\theta^E = \overline{C}_{12}^E \varepsilon_r + \overline{C}_{11}^E \varepsilon_\theta - \overline{e}_{31} E_z,$$

$$\tau_{r\theta}^E = \tfrac{1}{2}(\overline{C}_{11}^E - \overline{C}_{12}^E)\varepsilon_{r\theta},$$

$$\tau_{rz}^E = C_{55}^E \varepsilon_{rz} + e_{15} E_r,$$

$$\tau_{\theta z}^E = C_{55}^E \varepsilon_{\theta z} + e_{15} E_\theta, \tag{4a–e}$$

where the superscript E represents the variables in the piezoelectric material; $\overline{C}_{11}^E, \overline{C}_{12}^E$ and $\overline{e}_{31}$ are the reduced material constants of the piezoelectric medium for plane stress problems given by

$$\overline{C}_{12}^E = C_{12}^E - ((C_{13}^E)^2 / C_{33}^E),$$

$$\overline{C}_{11}^E = C_{11}^E - ((C_{13}^E)^2 / C_{33}^E),$$

$$\overline{e}_{31} = e_{31} - (C_{13}^E e_{33} / C_{33}^E), \tag{5a–c}$$

where $C_{11}^E, C_{12}^E, C_{13}^E, C_{33}^E$ and C_{55}^E are the module of elasticity under constant electric field, e_{31}, e_{33} and e_{15} are the piezoelectric constants, E_r, E_θ and E_z are the electric field intensities in the radial, tangential and transverse direction, respectively. These are given by

$$E_r = -\frac{\partial \phi}{\partial r}, \quad E_\theta = -\frac{\partial \phi}{r \partial \theta}, \quad E_z = -\frac{\partial \phi}{\partial z}, \tag{6a–c}$$

where ϕ is the electric potential at any point of the piezoelectric layers. The corresponding electric displacements D_r, D_θ and D_z are given by

$$D_r = e_{15} \varepsilon_{rz} + \Xi_{11} E_r,$$

$$D_\theta = e_{15} \varepsilon_{\theta z} + \Xi_{11} E_\theta,$$

$$D_z = \overline{e}_{31} (\varepsilon_r + \varepsilon_\theta) + \overline{\Xi}_{33} E_z, \tag{7a–c}$$

where $\overline{\Xi}_{33}$ is the reduced dielectric constant, Ξ_{11} and Ξ_{33} are the dielectric constants, all of the piezoelectric layer, and $\overline{\Xi}_{11} = \Xi_{11}, \overline{\Xi}_{33} = \Xi_{33} + e_{33}^2 / C_{33}^E$.

For free vibration analysis, a sinusoidal variation of the electrical potential in the transverse direction proposed by Liu et al. [20] and Duan et al. [21] is assumed, so that the potential function is written as

$$\phi = \begin{cases} \varphi(r, \theta, t) \sin\left(\dfrac{\pi(z-h)}{h_p}\right), & h \le z \le h + h_p, \\ \varphi(r, \theta, t) \sin\left(\dfrac{\pi(-z-h)}{h_p}\right), & -h - h_p \le z \le -h, \end{cases} \tag{8}$$

where $\varphi(r, \theta, t)$ is the electric potential on the mid-surface of the piezoelectric layer.

2.3. Basic equations

The resultant moments and shear forces can be expressed as follows:

$$M_i = \int_{-h}^{h} \sigma_i^h z \, dz + 2 \int_{h}^{h+h_p} \sigma_i^E z \, dz, \quad i = r, \theta, r\theta,$$

$$Q_i = \int_{-h}^{h} \sigma_{iz}^h \, dz + 2 \int_{h}^{h+h_p} \sigma_{iz}^E \, dz, \quad i = r, \theta, \tag{9a,b}$$

by substituting Eqs. (1)–(8) into (9a,b), the resultant bending moments, twisting moments and transverse shear forces, all per unit length in terms of ψ_r, ψ_θ, w and φ are written as

$$M_r = (D_1 + D_2) \frac{\partial \psi_r}{\partial r} + (D_1 + D_2 - 2A_1) \left(\frac{\psi_r}{r} + \frac{\partial \psi_\theta}{r \partial \theta} \right) - S_1 \left(\frac{\partial^2 w}{\partial r^2} + \frac{\partial w}{r \partial r} + \frac{\partial^2 w}{r^2 \partial \theta^2} \right) + S_2 \frac{\partial^2 w}{\partial r^2} - \frac{4}{\pi} h_p \overline{e}_{31} \varphi,$$

$$M_\theta = (D_1 + D_2 - 2A_1) \frac{\partial \psi_r}{\partial r} + (D_1 + D_2) \left(\frac{\psi_r}{r} + \frac{\partial \psi_\theta}{r \partial \theta} \right) - S_3 \left(\frac{\partial^2 w}{\partial r^2} + \frac{\partial w}{r \partial r} + \frac{\partial^2 w}{r^2 \partial \theta^2} \right) - S_2 \frac{\partial^2 w}{\partial r^2} - \frac{4}{\pi} h_p \overline{e}_{31} \varphi,$$

$$M_{r\theta} = A_1 \left(\frac{\partial \psi_r}{r \partial \theta} + \frac{\partial \psi_\theta}{\partial r} - \frac{\psi_\theta}{r} \right) + S_2 \left(\frac{\partial^2 w}{r \partial r \partial \theta} - \frac{\partial w}{r^2 \partial \theta} \right),$$

$$Q_r = A_2 \left(\frac{\partial w}{\partial r} + \psi_r \right) - \frac{4}{\pi} h_p e_{15} \frac{\partial \varphi}{\partial r},$$

$$Q_\theta = A_2 \left(\frac{\partial w}{r \partial \theta} + \psi_\theta \right) - \frac{4}{\pi} h_p e_{15} \frac{\partial \varphi}{r \partial \theta}, \tag{10a–e}$$

where the unknown constants in the above equations are given in Appendix A.

By obtaining the strain and kinetic energies of an annular Reddy plate with integrated piezoelectric layers and applying Hamilton principle, three equations of motion for dynamic behavior of a piezoelectric coupled annular Reddy plate can be found as follows

$$\frac{\partial M_r}{\partial r}+\frac{1}{r}\frac{\partial M_{r\theta}}{\partial\theta}+\frac{M_r-M_\theta}{r}-Q_r+c_1\left[\frac{1}{(h+h_p)^2}R_r-\frac{1}{3(h+h_p)^2}\left(\frac{\partial P_r}{\partial r}+\frac{1}{r}\frac{\partial P_{r\theta}}{\partial\theta}+\frac{P_r-P_\theta}{r}\right)\right]=m_3\ddot{\psi}_r-c_2m_5\frac{\partial\ddot{w}}{\partial r},$$

$$\frac{\partial M_{r\theta}}{\partial r}+\frac{\partial M_\theta}{r\partial\theta}+\frac{2M_{r\theta}}{r}-Q_\theta+c_1\left[\frac{1}{(h+h_p)^2}R_\theta-\frac{1}{3(h+h_p)^2}\left(\frac{\partial P_{r\theta}}{\partial r}+\frac{1}{r}\frac{\partial P_\theta}{\partial\theta}\right)-\frac{2}{3(h+h_p)^2}\frac{P_{r\theta}}{r}\right]=m_3\ddot{\psi}_\theta-c_2m_5\frac{1}{r}\frac{\partial\ddot{w}}{\partial\theta},$$

$$\frac{\partial Q_r}{\partial r}+\frac{1}{r}\frac{\partial Q_\theta}{\partial\theta}+\frac{Q_r}{r}+c_1\left[\frac{1}{3(h+h_p)^2}\left(\frac{\partial^2P_r}{\partial r^2}+\frac{2}{r}\frac{\partial^2P_{r\theta}}{\partial r\partial\theta}+\frac{1}{r^2}\frac{\partial^2P_\theta}{\partial\theta^2}\right)+\frac{1}{3(h+h_p)^2}\left(\frac{2}{r}\frac{\partial P_r}{\partial r}-\frac{1}{r}\frac{\partial P_\theta}{\partial r}+\frac{2}{r^2}\frac{\partial P_{r\theta}}{\partial\theta}\right)\right.$$
$$\left.-\frac{1}{(h+h_p)^2}\left(\frac{\partial R_r}{\partial r}+\frac{1}{r}\frac{\partial R_\theta}{\partial\theta}\right)-\frac{1}{(h+h_p)^2}\frac{R_r}{r}\right]=m_1\ddot{w}+c_1\left[m_5\left(\frac{\partial\ddot{\psi}_r}{\partial r}+\frac{1}{r}\frac{\partial\ddot{\psi}_\theta}{\partial\theta}+\frac{\ddot{\psi}_r}{r}\right)-m_7\left(\frac{\partial^2\ddot{w}}{\partial r^2}+\frac{1}{r}\frac{\partial\ddot{w}}{\partial r}+\frac{1}{r^2}\frac{\partial^2\ddot{w}}{\partial\theta^2}\right)\right].\tag{11a–c}$$

These equations are similar to those obtained by Nosier and Reddy [15].

In the Reddy's theory the tracers c_1 and c_2 are set equal to 1. The coefficients m_1, m_3, m_5 and m_7 are defined as

$$(I_1,I_2,I_3,I_4,I_5,I_7)=\int_{-h}^{h}\rho(1,z,z^2,z^3,z^4,z^6)\,\mathrm{d}z+2\int_{h}^{h+h_p}\rho_p(1,z,z^2,z^3,z^4,z^6)\,\mathrm{d}z,$$

$$m_1=I_1,\quad m_3=I_3-\frac{2}{3(h+h_p)^2}I_5+\frac{1}{9(h+h_p)^4}I_7,$$

$$m_5=\frac{1}{3(h+h_p)^2}\left(I_5-\frac{1}{3(h+h_p)^2}I_7\right),\quad m_7=\frac{1}{9(h+h_p)^4}I_7,\tag{12a–e}$$

in which, ρ and ρ_p are the material densities of the host material and piezoelectric layer, respectively. The equations of motion of the plate according to FSDT are also obtained by letting $c_1=c_2=0$, $m_1=I_1$ and $m_3=I_3$ in Eqs. (11a–c).

Levinson's theory obtained by taking $c_1=0$ and $c_2=1$ in Eqs. (11a–c) and coefficients m_1, m_3 and m_5 are defined as

$$m_1=I_1,\quad m_3=I_3-\frac{1}{3(h+h_p)^2}I_5,\quad m_5=\frac{1}{3(h+h_p)^2}I_5,\tag{13a–c}$$

therefore, the governing equation of motion for the Levinson plate in absence of the applied load and assumption of the free harmonic motion in terms of the stress resultants are given by

$$\frac{\partial M_r}{\partial r}+\frac{1}{r}\frac{\partial M_{r\theta}}{\partial\theta}+\frac{M_r-M_\theta}{r}-Q_r=\bar{I}_3\ddot{\psi}_r-\frac{1}{3(h+h_p)^2}I_5\frac{\partial\ddot{w}}{\partial r},$$

$$\frac{\partial M_{r\theta}}{\partial r}+\frac{\partial M_\theta}{r\partial\theta}+\frac{2M_{r\theta}}{r}-Q_\theta=\bar{I}_3\ddot{\psi}_\theta-\frac{1}{3(h+h_p)^2}I_5\frac{1}{r}\frac{\partial\ddot{w}}{\partial\theta},$$

$$\frac{\partial Q_r}{\partial r}+\frac{1}{r}\frac{\partial Q_\theta}{\partial\theta}+\frac{Q_r}{r}=I_1\ddot{w},\tag{14a–c}$$

where

$$\bar{I}_3=I_3-\frac{1}{3(h+h_p)^2}I_5,\tag{15}$$

substituting Eqs. (10a–e) into (14a–c) gives three partial differential equation, namely

$$(D_1+D_2)\left(\frac{\partial^2\psi_r}{\partial r^2}+\frac{\partial\psi_r}{r\partial r}-\frac{\psi_r}{r^2}+\frac{\partial^2\psi_\theta}{r\partial r\partial\theta}-\frac{\partial\psi_\theta}{r^2\partial\theta}\right)+A_1\left(\frac{\partial^2\psi_r}{r^2\partial\theta^2}-\frac{\partial\psi_\theta}{r^2\partial\theta}-\frac{\partial^2\psi_\theta}{r\partial r\partial\theta}\right)-A_2\left(\frac{\partial w}{\partial r}+\psi_r\right)+A_3\frac{\partial\varphi}{\partial r}-S_3\frac{\partial(\Delta w)}{\partial r}=\bar{I}_3\ddot{\psi}_r-\frac{1}{3(h+h_p)^2}I_5\frac{\partial\ddot{w}}{\partial r},$$

$$(D_1+D_2)\left(\frac{\partial^2\psi_r}{r\partial r\partial\theta}+\frac{\partial^2\psi_\theta}{r^2\partial\theta^2}+\frac{\partial\psi_r}{r^2\partial\theta}\right)+A_1\left(-\frac{\partial^2\psi_r}{r\partial r\partial\theta}+\frac{\partial\psi_r}{r^2\partial\theta}+\frac{\partial^2\psi_\theta}{\partial r^2}-\frac{\psi_\theta}{r^2}+\frac{\partial\psi_\theta}{r\partial r}\right)-A_2\left(\frac{\partial w}{r\partial\theta}+\psi_\theta\right)+A_3\frac{\partial\varphi}{r\partial\theta}-S_3\frac{\partial(\Delta w)}{r\partial\theta}=\bar{I}_3\ddot{\psi}_\theta-\frac{1}{3(h+h_p)^2}I_5\frac{1}{r}\frac{\partial\ddot{w}}{\partial\theta},$$

$$A_2\Delta w+A_2\left(\frac{\partial\psi_r}{\partial r}+\frac{\partial\psi_\theta}{r\partial\theta}+\frac{\psi_r}{r}\right)-\frac{4}{\pi}h_pe_{15}\Delta\varphi=I_1\ddot{w},\tag{16a–c}$$

where Δ is the Laplace operator in the polar coordinate given by

$$\Delta=\frac{\partial^2}{\partial r^2}+\frac{\partial}{r\partial r}+\frac{\partial^2}{r^2\partial\theta^2}.\tag{17}$$

Note that all of the electrical variables primarily must satisfy Maxwell's equation which requires that the divergence of the electric flux density vanishes at any point within the media. This condition can be satisfied approximately by enforcing the integration of the electric flux divergence across the thickness of the piezoelectric layers to be zero for any r and θ as

$$\int_h^{h+h_p}\left(\frac{\partial(rDr)}{r\partial r}+\frac{\partial D_\theta}{r\partial\theta}+\frac{\partial D_z}{\partial z}\right)\mathrm{d}z=0, \tag{18}$$

substituting Eqs. (7a–c) into above equation and simplifying the result gives

$$\left(\frac{\partial\psi_r}{\partial r}+\frac{\partial\psi_\theta}{r\partial\theta}+\frac{\psi_r}{r}\right)+A_4\Delta w-A_5\Delta\varphi+A_6\varphi=0, \tag{19}$$

where the unknown constants in the above equations are given in Appendix A.

3. Analysis of a piezoelectric coupled annular plate

3.1. Determination of the transverse displacement (w)

In order to solve four complex differential equations of motion, following steps must be taken so that Eqs. (16a–c) and (19) become uncoupled:

1. Eq. (16a) is first differentiated with respect to r.
2. Eq. (16a) is divided by r.
3. Eq. (16b) is first differentiated with respect to θ and then divided by r.
4. An auxiliary function is defined as

$$\Psi=\frac{\partial\psi_r}{\partial r}+\frac{1}{r}\frac{\partial\psi_\theta}{\partial\theta}+\frac{\psi_r}{r}. \tag{20}$$

5. If three equations obtained from steps (1) and (2) and (3) are added together, we will obtain

$$(D_1+D_2)\Delta\Psi-A_2\Delta w-A_2\Psi+A_3\Delta\varphi-S_3\Delta\Delta w=\bar{I}_3\ddot{\Psi}-\frac{1}{3(h+h_p)^2}I_5\Delta\ddot{w}, \tag{21}$$

6. Eqs. (16c) and (19) must be rewritten by using Eq. (20) as

$$A_2\Delta w+A_2\Psi-\frac{4}{\pi}h_pe_{15}\Delta\varphi=I_1\ddot{w},$$

$$\Psi+A_4\Delta w-A_5\Delta\varphi+A_6\varphi=0, \tag{22a,b}$$

7. The next step in the analysis is to eliminate the parameters Ψ and φ between Eqs. (21), (22a) and (22b). After some mathematical manipulation, the obtained equation is uncoupled from φ, ψ_r and ψ_θ.

An uncoupled sixth-order partial differential equation with constant coefficients is acquired in terms of w as follow

$$P_1\Delta\Delta\Delta w+P_2\Delta\Delta\Delta\ddot{w}+P_3\Delta\Delta w+P_4\Delta\Delta\ddot{w}+P_5\Delta\Delta\overset{(4)}{w}+P_6\Delta\overset{(4)}{w}+P_7\Delta\ddot{w}+P_8\overset{(4)}{w}+P_9\ddot{w}=0, \tag{23}$$

where the coefficients, P_1, P_2, P_3, P_4, P_5, P_6, P_7, P_8 and P_9, are given in Appendix A.

The solution of $w(r,\theta,t)$ for wave propagation in the circumferential direction can be written as

$$w(r,\theta,t)=\overline{w}(r)\cos(p\theta)\exp(\mathrm{i}\omega t), \tag{24}$$

where $\overline{w}(r)$ is the amplitude of the z-direction displacement as a function of radial distance only; ω is the natural frequency of the plate; and non-negative integer p represents the circumferential wave number of the corresponding mode shape. Rewriting Eq. (23) in terms of $\overline{w}(r)$ and canceling the $\exp(\mathrm{i}\omega t)$ term gives a differential equation, namely

$$(P_1-P_2\omega^2)\overline{\Delta\Delta\Delta}\overline{w}+(P_3-P_4\omega^2+P_5\omega^4)\overline{\Delta\Delta}\overline{w}+(P_6\omega^4-P_7\omega^2)\overline{\Delta}\overline{w}+(P_8\omega^4-P_9\omega^2)\overline{w}=0, \tag{25}$$

where the operator $\overline{\Delta}$ is given by

$$\overline{\Delta}=\frac{\partial^2}{\partial r^2}+\frac{\partial}{r\partial r}-\frac{p^2}{r^2}. \tag{26}$$

Transforming Eq. (25) into the form

$$(\overline{\Delta}-x_1)(\overline{\Delta}-x_2)(\overline{\Delta}-x_3)\overline{w}=0, \tag{27}$$

where x_1, x_2 and x_3 are the three roots of the following cubic equation:

$$(P_1-P_2\omega^2)x^3+(P_3-P_4\omega^2+P_5\omega^4)x^2+(P_6\omega^4-P_7\omega^2)x+(P_8\omega^4-P_9\omega^2)=0. \tag{28}$$

The general solution to Eq. (25) may be expressed as

$$\overline{w} = \overline{w}_1 + \overline{w}_2 + \overline{w}_3, \tag{29}$$

in which $\overline{w}_i$ $(i=1,2,3)$ are obtained by three different kinds of Bessel's equations as follow

$$(\overline{\Delta} - x_1)\overline{w}_1 = 0,$$

$$(\overline{\Delta} - x_2)\overline{w}_2 = 0,$$

$$(\overline{\Delta} - x_3)\overline{w}_3 = 0, \tag{30a–c}$$

the second order term of Eq. (28) can easily be eliminated by using the following transformation

$$x = y - (P_3 - P_4\omega^2 + P_5\omega^4)/3(P_1 - P_2\omega^2), \tag{31}$$

thus, Eq. (28) reduced to

$$y^3 + by + c = 0, \tag{32}$$

where

$$b = \frac{P_6\omega^4 - P_7\omega^2}{P_1 - P_2\omega^2} - \frac{(P_3 - P_4\omega^2 + P_5\omega^4)^2}{3(P_1 - P_2\omega^2)^2}, \tag{33a}$$

$$c = \frac{P_8\omega^4 - P_9\omega^2}{P_1 - P_2\omega^2} - \frac{\omega^2(P_3 - P_4\omega^2 + P_5\omega^4)(P_6\omega^2 - P_7)}{3(P_1 - P_2\omega^2)^2} + \frac{2(P_3 - P_4\omega^2 + P_5\omega^4)^3}{27(P_1 - P_2\omega^2)^3}. \tag{33b}$$

It is well know that the discriminant of a third-order equation can be expressed as

$$\eta = \left(\frac{c}{2}\right)^2 + \left(\frac{b}{3}\right)^3, \tag{34}$$

the parameter η practically takes negative values ($\eta < 0$). Therefore, based on Cardano's formula [24], three distinct real roots of Eq. (28) are given by

$$x_1 = 2S\cos\frac{\gamma}{3} - \frac{P_3 - P_4\omega^2 + P_5\omega^4}{3(P_1 - P_2\omega^2)},$$

$$x_2 = 2S\cos\frac{\gamma + 2\pi}{3} - \frac{P_3 - P_4\omega^2 + P_5\omega^4}{3(P_1 - P_2\omega^2)},$$

$$x_3 = 2S\cos\frac{\gamma + 4\pi}{3} - \frac{P_3 - P_4\omega^2 + P_5\omega^4}{3(P_1 - P_2\omega^2)}, \tag{35a–c}$$

where

$$S = \frac{1}{3}\sqrt{\frac{(P_3 - P_4\omega^2 + P_5\omega^4)^2 - 3(P_1 - P_2\omega^2)(P_6\omega^4 - P_7\omega^2)}{(P_1 - P_2\omega^2)^2}}, \quad \gamma = \arccos\left[-\frac{c}{2\sqrt{\left(\frac{-b}{3}\right)^3}}\right]. \tag{36a,b}$$

Therefore, the solution of Eq. (25) can be expressed as

$$\overline{w}(r) = \sum_{i=1}^{3}[c_i w_{i1}(p, \chi_i r) + c_{i+3} w_{i2}(p, \chi_i r)], \tag{37}$$

where

$$\chi_i = \sqrt{|x_i|}, \tag{38}$$

and

$$w_{i1}(p, \chi_i r) = \begin{cases} J_p(\chi_i r), & x_i < 0, \\ I_p(\chi_i r), & x_i > 0, \end{cases} \quad i = 1,2,3,$$

$$w_{i2}(p, \chi_i r) = \begin{cases} Y_p(\chi_i r), & x_i < 0, \\ K_p(\chi_i r), & x_i > 0, \end{cases} \quad i = 1,2,3, \tag{39a,b}$$

in which J_p and Y_p are Bessel functions of the first and second kind, respectively, I_p and K_p are modified Bessel functions of the first and second kind, respectively and c_i $(i=1,2,\ldots,6)$ are constants of integration.

3.2. Determination of electric potential in the piezoelectric layer

The solution of $\varphi(r,\theta,t)$ for wave propagation in the circumferential direction can be written as

$$\varphi(r,\theta,t)=\overline{\varphi}(r)\cos(p\theta)\exp(\mathrm{i}\omega t), \tag{40}$$

substituting Eqs. (40) and (24) into (21), (22a) and (22b), eliminating Ψ from these equations; and canceling the $\exp(\mathrm{i}\omega t)$ term give a relation between $\overline{\varphi}(r)$ and $\overline{w}(r)$, namely

$$\overline{\varphi}=\frac{K_2}{K_1}\overline{\Delta\Delta}\overline{w}+\frac{K_3}{K_1}\overline{\Delta}\overline{w}+\frac{K_4}{K_1}\overline{w}, \tag{41}$$

where the coefficients, K_1, K_2, K_3 and K_4, are given in Appendix A.

From Eqs. (30a–c) we can write following equations:

$$\overline{\Delta\Delta}\overline{w}_i=x_i^2\overline{w}_i,\quad \overline{\Delta}\overline{w}_i=x_i\overline{w}_i,\quad i=1,2,3 \tag{42a,b}$$

the electric potential can be expressed as follows by substituting Eq. (42) into (41):

$$\overline{\varphi}(r)=\sum_{i=1}^{3}L_i\overline{w}_i(r), \tag{43}$$

where

$$L_i=\frac{K_2}{K_1}x_i^2+\frac{K_3}{K_1}x_i+\frac{K_4}{K_1},\quad i=1,2,3. \tag{44}$$

3.3. Determination of ψ_r and ψ_θ

In order to determine the slope rotations ψ_r and ψ_θ, the following forms are initially considered

$$\psi_r=a_1\frac{\partial w_1}{\partial r}+a_2\frac{\partial w_2}{\partial r}+a_3\frac{\partial w_3}{\partial r}+a_4\frac{\partial w_4}{r\partial\theta},$$

$$\psi_\theta=b_1\frac{\partial w_1}{r\partial\theta}+b_2\frac{\partial w_2}{r\partial\theta}+b_3\frac{\partial w_3}{r\partial\theta}+b_4\frac{\partial w_4}{\partial r}, \tag{45a,b}$$

where $a_i,b_i\,(i=1,2,3,4)$ are unknown coefficients. The function w_4 is also unknown and must be determined. The unknowns a_i,b_i and w_4 can be obtained as follows by substituting Eqs. (45a,b) into (16a–c):

$$a_i=b_i=\frac{A_2+\dfrac{I_5\omega^2}{3(h+h_p)^2}-A_3L_i+S_3x_i}{\overline{I}_3\omega^2-A_2+(D_1+D_2)x_i},\quad i=1,2,3,\quad a_4=1,\quad b_4=-1 \tag{46a–d}$$

and the function w_4 take the following form

$$w_4(r,\theta,t)=\overline{w}_4(r)\sin(p\theta)\exp(\mathrm{i}\omega t),$$

$$\overline{w}_4(r)=c_7w_{41}(p,\chi_4r)+c_8w_{42}(p,\chi_4r), \tag{47a,b}$$

where

$$x_4=\frac{A_2-\overline{I}_3\omega^2}{A_1},$$

$$\chi_4=\sqrt{|x_4|},$$

$$w_{41}(p,\chi_4r)=\begin{cases}J_p(\chi_4r), & x_4<0,\\ I_p(\chi_4r), & x_4>0,\end{cases}$$

$$w_{42}(p,\chi_4r)=\begin{cases}Y_p(\chi_4r), & x_4<0,\\ K_p(\chi_4r), & x_4>0.\end{cases} \tag{48a–d}$$

If the plate is insulated at the edge, the electrical flux conservation equation is given by

$$\int_h^{h+h_p}D_r(r,\theta,t)\,\mathrm{d}z=0, \tag{49}$$

substituting Eq. (7a) into (49) yields the electric boundary condition

$$\frac{h_p(3h+2h_p)e_{15}}{(h+h_p)^2}\left(\psi_r+\frac{\partial w}{\partial r}\right)-\frac{6\Xi_{11}}{\pi}\frac{\partial\varphi}{\partial r}=0. \tag{50}$$

The standard boundary conditions for the clamped and simply supported (hard and soft types) ends are given respectively as follows:

(1) Clamped

$$w(r_1,\theta,t)=\psi_r(r_1,\theta,t)=\psi_\theta(r_1,\theta,t)=\left[\frac{h_p(3h+2h_p)e_{15}}{(h+h_p)^2}\left(\psi_r+\frac{\partial w}{\partial r}\right)-\frac{6\Xi_{11}}{\pi}\frac{\partial\varphi}{\partial r}\right]_{r=r_1}=0,$$

$$w(r_0,\theta,t)=\psi_r(r_0,\theta,t)=\psi_\theta(r_0,\theta,t)=\left[\frac{h_p(3h+2h_p)e_{15}}{(h+h_p)^2}\left(\psi_r+\frac{\partial w}{\partial r}\right)-\frac{6\Xi_{11}}{\pi}\frac{\partial\varphi}{\partial r}\right]_{r=r_0}=0. \tag{51a–h}$$

(2) Simply supported (hard type)

$$w(r_1,\theta,t)=\psi_\theta(r_1,\theta,t)=M_r(r_1,\theta,t)=\left[\frac{h_p(3h+2h_p)e_{15}}{(h+h_p)^2}\left(\psi_r+\frac{\partial w}{\partial r}\right)-\frac{6\Xi_{11}}{\pi}\frac{\partial\varphi}{\partial r}\right]_{r=r_1}=0,$$

$$w(r_0,\theta,t)=\psi_\theta(r_0,\theta,t)=M_r(r_0,\theta,t)=\left[\frac{h_p(3h+2h_p)e_{15}}{(h+h_p)^2}\left(\psi_r+\frac{\partial w}{\partial r}\right)-\frac{6\Xi_{11}}{\pi}\frac{\partial\varphi}{\partial r}\right]_{r=r_0}=0. \tag{52a–h}$$

(3) Simply supported (soft type)

$$w(r_1,\theta,t)=M_r(r_1,\theta,t)=M_{r\theta}(r_1,\theta,t)=\left[\frac{h_p(3h+2h_p)e_{15}}{(h+h_p)^2}\left(\psi_r+\frac{\partial w}{\partial r}\right)-\frac{6\Xi_{11}}{\pi}\frac{\partial\varphi}{\partial r}\right]_{r=r_1}=0,$$

$$w(r_0,\theta,t)=M_r(r_0,\theta,t)=M_{r\theta}(r_0,\theta,t)=\left[\frac{h_p(3h+2h_p)e_{15}}{(h+h_p)^2}\left(\psi_r+\frac{\partial w}{\partial r}\right)-\frac{6\Xi_{11}}{\pi}\frac{\partial\varphi}{\partial r}\right]_{r=r_0}=0. \tag{53a–h}$$

It should be noted that at the edge of the plate with hard simply supported boundary condition, normal to mid-plane cannot rotate in the $z-\theta$ plane, therefore ψ_θ is equal to zero at the plate edge. According to the displacement field as ψ_θ becomes zero, the edge of the plate will be constrained in circumferential direction, while the edge of the plate with soft simply supported boundary condition can move in circumferential directions.

Natural frequencies of annular plates can be calculated by using above boundary condition. Closed-form characteristic equations of annular plates under different boundary conditions are given in detail in Appendix B

4. Comparison studies

For convenience of notation, an annular plate is described by a symbolism defining the boundary conditions at their edges, For example, C–S denotes an annular plate with clamped edge on the inner radius and simply supported (soft type) on the outer radius. It should be noted that in this paper soft simply supported and hard simply supported boundary conditions are denoted by S and S*, respectively and the material properties are listed in Table 1.

For verification of the present formulation, a comparison study of the results for thick annular plates without piezoelectric layer for F–F, F–S, and F–C boundary conditions is made with the results from Mindlin theory given by Irie

Table 1
Material properties.

Property	Host structure	PZT4	PIC-151	PZT(NEPEC6)
Young's modulus (Gpa)	$E=200$	$C_{11}^E=132$ $C_{12}^E=71$ $C_{33}^E=115$ $C_{13}^E=73$ $C_{55}^E=26$	$C_{11}^E=107.6$ $C_{12}^E=63.13$ $C_{33}^E=100.4$ $C_{13}^E=63.86$ $C_{55}^E=19.62$	$C_{11}^E=139$ $C_{12}^E=77.8$ $C_{33}^E=115$ $C_{13}^E=74.3$ $C_{55}^E=25.6$
Poisson ratio	0.3	–	–	–
Mass density (kg/m^3)	7800	7500	7800	7600
e_{31} (C/m^2)	–	-4.1	-9.52	-5.2
e_{33} (C/m^2)	–	14.1	15.14	15.1
e_{15} (C/m^2)	–	10.5	11.97	12.7
Ξ_{11} (nF/m)	–	7.124	9.837	6.463
Ξ_{33} (nF/m)	–	5.841	8.190	5.622

Table 2
Comparison of non-dimensional frequencies ($\lambda = \omega r_0^2 \sqrt{2\rho h/D}$) of the moderately thick annular plates for different boundary conditions when $r_1/r_0 = 0.1$ and $h/r_0 = 0.15$.

BC[a]	Method	Mode types (p,n)					
		(0,0)	(0,1)	(1,0)	(1,1)	(2,0)	(2,1)
F–F	Present	7.83486	26.6297	15.586	34.4198	4.81416	24.3429
	Ref. [2]	7.83	26.58	15.7	34.62	4.81	24.12
	Ref. [4]	7.8544	26.865	15.824	35.170	4.8172	24.403
	Ref. [5][b]	7.83027	26.57574	15.69685	34.62412	4.80672	24.12241
F–S*	Present	4.54104	21.7132	11.5223	30.1501	19.0852	40.078
	Ref. [2]	4.54	21.67	11.5	30.05	19.04	39.93
	Ref. [4]	4.5572	21.933	11.602	30.565	19.279	40.757
	Ref. [5][b]	4.53849	21.66535	11.50426	30.05296	19.04346	39.93500
F–C	Present	8.18546	24.1273	14.6602	31.7018	21.5359	41.1290
	Ref. [2]	8.37	24.7	15.01	32.23	22.02	41.64
	Ref. [4]	8.4771	25.203	15.274	32.982	22.461	42.734
	Ref. [5][b]	8.36584	24.70209	15.01476	32.23117	22.01586	41.64170

$D = E(2h)^3/12(1-\nu^2)$ is flexural rigidity of host plate.
[a] *Note*: BC means Boundary Conditions.
[b] Shear correction factor $=\pi^2/12$.

Table 3
Comparison of frequencies ω (rad/s) of the piezoelectric coupled thin annular plates under different boundary conditions when $h/r_0 = 1/60$.

BC	p	n	Present (LPT)	IPT [21]	FEM [22]	Diff (%)	
						LPT and IPT	LPT and FEM
C–C	0	0	2764.83	2769	2724	−0.15	1.50
		1	7499.30	7517	7418	−0.24	1.10
		2	14 383.1	14 428	14 289	−0.31	0.66
	1	0	2894.71	2899	2853	−0.15	1.46
		1	7724.79	7743	7642	−0.24	1.08
		2	14 652.3	14 698	14 557	−0.31	0.65
	2	0	3432.56	3438	3381	−0.16	1.52
		1	8487.97	8507	8394	−0.22	1.12
		2	15 520.4	15 566	15 416	−0.29	0.68
C–S	0	0	1821.69	1823	1790	−0.07	1.77
		1	6058.15	6066	5967	−0.13	1.53
		2	12 502.1	12 523	12 357	−0.17	1.17
	1	0	1955.61	1957	1922	−0.07	1.75
		1	6280.92	6289	6187	−0.13	1.52
		2	12 773.3	12 794	12 625	−0.16	1.17
	2	0	2493.81	2495	2448	−0.05	1.87
		1	7042.74	7050	6934	−0.10	1.57
		2	13 651.7	13 672	13 490	−0.15	1.20
S–C	0	0	2193.20	2194	2152	−0.04	1.91
		1	6449.77	6455	6345	−0.08	1.65
		2	12 918.6	12 934	12 755	−0.12	1.28
	1	0	2396.72	2397	2352	−0.01	1.90
		1	6770.0	6774	6663	−0.06	1.61
		2	13 277.6	13 293	13 112	−0.12	1.26
	2	0	3158.33	3159	3102	−0.02	1.82
		1	7810.24	7815	7692	−0.06	1.54
		2	14 412.5	14 428	14 243	−0.11	1.19
S–S	0	0	1388.45	1388	1358	0.03	2.24
		1	5116.43	5115	5014	0.03	2.04
		2	11 115.9	11 114	10 921	0.02	1.78
	1	0	1584.45	1583	1551	0.09	2.16
		1	5434.51	5433	5328	0.03	2.00
		2	11 480.9	11 478	11 283	0.03	1.75
	2	0	2307.54	2306	2260	0.07	2.10
		1	6470.48	6468	6348	0.04	1.93
		2	12 635.6	12 632	12 428	0.03	1.67

et al. [2], Efraim and Eisenberger [5], and with the 3-D elasticity analysis by Liew and Yang [4]. These are presented in Table 2. The results are also listed in these tables for three circumferential wave numbers (p=0,1 and 2) while the first two modes (n=0 and 1) are considered for each value of p. It is evident from Table 2 that the present solution is in good agreement with these three references, and results obtained on the basis of the 3-D Ritz method [4] are greater than those of the present LPT. This is attributed to the fact that natural frequencies by the Ritz method are upper bounds of the exact ones.

An interesting comparison study of the natural frequencies of the present method with those of Duan et al. [21] using the analytical solution based on the improved plate theory (IPT) and Liu et al. [22] using the finite element method are listed in Tables 3 and 4. In these tables, two different thickness-radius ratios ($h/r_0=1/60$ and $1/20$) are examined, which correspond to thin and moderately thick plates, respectively. The material of host plate is steel and that of the piezoelectric layer is PZT4. The inner radius (r_1) and outer radius (r_0) of the annular plate are 0.1 and 0.6 m, respectively. The thickness ratio of the piezoelectric layer to the host plate is 1/10. The percentage difference given in Tables 3 and 4 is defined as follows:

$$\%\text{Diff}=\frac{[(\text{LPT})-(\text{others methods})]}{(\text{others methods})}\times 100.$$

It is observed from Tables 3 and 4 that all results obtained on the basis of the present solution are always higher than those of FEM [22] and also frequencies derived from present LPT are lower than those of the IPT [21] under all the four boundary conditions except S–S. The agreement between the present results and those given by Duan et al. [21] is found to be excellent. Good agreement is also achieved between the present results and those of Liu et al. [22]. It is worth noting

Table 4
Comparison of frequencies ω (rad/s) of the piezoelectric coupled thick annular plates under different boundary conditions when $h/r_0=1/20$.

BC	p	n	Present (LPT)	IPT [21]	FEM [22]	Diff (%) LPT and IPT	Diff (%) LPT and FEM
C–C	0	0	7335.11	7416	7435	−1.09	−1.34
		1	17 985.2	18 235	18 515	−1.37	−2.86
		2	31 423.2	31 869	32 692	−1.40	−3.88
	1	0	7644.76	7728	7746	−1.08	−1.31
		1	18 530.3	18 774	19 050	−1.30	−2.73
		2	32 035.2	32 468	33 291	−1.33	−3.77
	2	0	9093.99	9169	9172	−0.82	−0.85
		1	20 419.1	20 639	20 912	−1.07	−2.36
		2	34 000.2	34 397	35 233	−1.15	−3.50
C–S	0	0	5030.66	5064	5031	−0.66	−0.01
		1	15 376.7	15 500	15 531	−0.80	−0.99
		2	28 967.1	29 201	29 489	−0.80	−1.77
	1	0	5372.2	5406	5369	−0.63	0.06
		1	15 933.8	16 048	16 070	−0.71	−0.85
		2	29 608.8	29 827	30 104	−0.73	−1.64
	2	0	6886.9	6907	6838	−0.29	0.72
		1	17 903.1	17 986	17 978	−0.46	−0.42
		2	31 678.7	31 854	32 110	−0.55	−1.34
S–C	0	0	6107.77	6125	6045	−0.28	1.04
		1	16 445.5	16 536	16 469	−0.55	−0.14
		2	29 993.5	30 197	30 325	−0.67	−1.09
	1	0	6537.33	6555	6479	−0.27	0.90
		1	17 077.1	17 172	17 126	−0.55	−0.29
		2	30 616.2	30 826	31 000	−0.68	−1.24
	2	0	8495.33	8528	8470	−0.38	0.30
		1	19 338.7	19 453	19 496	−0.59	−0.81
		2	32 729.5	32 959	33 291	−0.70	−1.69
S–S	0	0	4002.60	3997	3912	0.14	2.32
		1	13 784.9	13 775	13 547	0.07	1.76
		2	27 430.3	27 430	27 117	0.00	1.16
	1	0	4457.99	4450	4361	0.18	2.22
		1	14 452.4	14 443	14 223	0.07	1.61
		2	28 098.2	28 102	27 822	−0.01	0.99
	2	0	6437.99	6433	6332	0.08	1.67
		1	16 861.2	16 859	16 688	0.01	1.04
		2	30 365.6	30 385	30 222	−0.06	0.48

that the discrepancy of the frequencies between the present results and those by the IPT [21] is greater for larger n (number of nodal circles) except S–S and in comparison with FEM [22] in Table 3 this trend is vice versa.

5. Results and discussion

In this section, natural frequencies of the piezoelectric coupled annular plates are presented in tabular and graphical forms for different plate and piezoelectric parameters. In all the computations, unless otherwise stated, the outer radius is 0.6 m and the material for the host plate is steel and that of the piezoelectric layer is PZT4 which their properties are listed in Table 1.

5.1. Effect of the plate parameters on the natural frequency

The frequencies ω (rad/s) of annular Levinson plates with three combinations of boundary conditions (C–C, S*–S* and S–S) and thickness to radius ratios ($h/r_0 = 1/60, 1/30$ and $1/10$) are listed in Table 5. Furthermore, in Table 6, a similar analysis of the frequencies ω (rad/s) is carried out for C–S*, C–S and S–C of annular Levinson plates with three different thickness to radius ratios ($h/r_0 = 1/30, 1/20$ and $1/10$).

In these tables, two different inner–outer radius ratios $r_1/r_0 = 0.1$ and 0.5 are examined. It is obvious from Tables 5 and 6 that regardless of the boundary conditions at the plate edges, the natural frequencies ω increases as the thickness to radius ratio h/r_0 or/and inner–outer radius ratio r_1/r_0 increases. As expected, the natural frequencies increases as the

Table 5
Frequencies ω (rad/s) of annular plates under C–C, S*–S* and S–S boundary conditions with piezoelectric layers when h/h_p=5.

P	n	$h/r_0 = 1/60$		$h/r_0 = 1/30$		$h/r_0 = 1/10$	
		$r_1/r_0 = 0.1$	$r_1/r_0 = 0.5$	$r_1/r_0 = 0.1$	$r_1/r_0 = 0.5$	$r_1/r_0 = 0.1$	$r_1/r_0 = 0.5$
C–C annular plates							
0	0	2307.71	7364.11	4420.91	13 278.4	9734.19	23 131.2
	1	6277.50	19 432.0	11 573.0	32 150.1	21 961.8	47 502.6
	2	12 109.0	36 155.0	21 418.0	55 625.1	36 781.2	77 399.8
	3	19 598.2	56 396.0	33 226.6	81 769.5	52 878.7	83 993.8
1	0	2438.91	7441.16	4653.35	13 405.5	10 465.7	23 355.8
	1	6538.08	19 536.0	12 045.8	32 315.0	23 388.4	47 833.3
	2	12 445.2	36 262.1	22 020.1	55 784.2	38 293.0	77 637.8
	3	19 983.8	56 500.4	33 905.1	81 917.2	54 308.7	84 871.8
2	0	3091.16	7685.73	5930.91	13 816.3	13 680.7	24 137.9
	1	7516.62	19 851.5	13 897.5	32 817.0	27 497.1	48 822.7
	2	13 618.5	36 585.1	24 155.7	56 264.4	42 522.2	78 375.3
	3	21 277.0	56 814.2	36 170.0	82 361.1	58 356.4	87 339.0
S–S* annular plates*							
0	0	1237.67	3407.83	2437.22	6637.41	6367.01	16 163.6
	1	4389.80	13 162.7	8460.41	24 098.7	19 414.3	45 505.2
	2	9454.90	28 417.3	17 643.0	48 306.9	35 328.6	76 769.5
	3	16 316.5	48 076.4	29 297.2	76 128.8	52 313.6	78 937.7
1	0	1433.14	3555.79	2822.76	6918.62	7476.37	16 751.4
	1	4786.79	13 317.0	9211.21	24 360.3	21 070.3	45 883.3
	2	9973.83	28 563.6	18 566.4	48 525.9	36 956.9	77 034.1
	3	16 899.1	48 211.1	30 264.9	76 310.3	53 773.3	79 066.9
2	0	2214.13	4001.41	4351.65	7762.13	11 273.3	18 477.5
	1	6057.69	13 780.2	11 583.6	25 142.9	25 704.1	47 007.3
	2	11 565.5	29 002.3	21 360.1	49 181.5	41 482.3	77 821.0
	3	18 671.3	48 615.0	33 173.1	76 853.9	57 911.3	79 535.6
S–S annular plates							
0	0	1237.67	3407.83	2437.22	6637.41	6367.01	16 163.6
	1	4389.80	13 162.7	8460.41	24 098.7	19 414.3	45 505.2
	2	9454.90	28 417.3	17 643.0	48 306.9	35 328.6	76 769.5
	3	16 316.5	48 076.4	29 297.2	76 128.8	52 313.6	78 937.7
1	0	1408.48	3545.30	2728.27	6879.32	7029.45	16 542.3
	1	4740.72	13 306.1	9050.67	24 325.1	20 600.3	45 760.0
	2	9912.28	28 553.3	18 373.8	48 497.6	36 582.8	76 910.9
	3	16 828.2	48 201.8	30 066.1	76 287.7	53 495.2	77 662.2
2	0	2192.66	3964.98	4276.11	7626.65	10 951.6	17 803.0
	1	5999.11	13 738.7	11 396.6	25 009.6	25 215.9	46 562.1
	2	11 456.9	28 962.3	21 046.9	49 071.7	40 888.9	77 427.9
	3	18 514.8	48 578.4	32 766.2	76 765.3	57 280.6	77 847.6

Table 6
Frequencies ω (rad/s) of annular plate under C–S*, C–S and S–C boundary conditions with piezoelectric layers when h/h_p=25.

p	n	$h/r_0=1/30$		$h/r_0=1/20$		$h/r_0=1/10$	
		$r_1/r_0=0.1$	$r_1/r_0=0.5$	$r_1/r_0=0.1$	$r_1/r_0=0.5$	$r_1/r_0=0.1$	$r_1/r_0=0.5$
C–S annular plates*							
0	0	2927.38	9379.51	4200.01	12 853.7	6979.96	18 804.5
	1	9497.97	27 870.1	13 123.0	35 549.5	19 900.2	46 479.3
	2	19 005.5	51 831.5	25 255.7	62 786.5	35 544.8	77 232.5
	3	30 762.2	78 943.5	39 460.8	92 333.4	52 440.9	80 291.1
1	0	3170.13	9552.65	4550.06	13 088.0	7818.49	19 207.2
	1	9960.61	28 060.0	13 813.5	35 792.5	21 410.9	46 830.0
	2	19 614.4	52 009.9	26 160.9	63 003.3	37 172.3	77 503.2
	3	31 458.1	79 103.9	40 459.4	92 518.2	53 931.5	84 413.2
2	0	44 14.43	10 098.0	64 14.20	13 831.6	11 322.7	20 467.7
	1	11 809.6	28 637.3	16 495.2	36 530.9	25 843.9	47 880.8
	2	21 796.9	52 547.5	29 210.1	63 655.1	41 677.6	78 311.3
	3	33 796.9	79 585.6	43 598.5	93 072.4	58 135.5	83 624.2
C–S annular plates							
0	0	2927.38	9379.51	4200.01	12 853.7	6979.96	18 804.5
	1	9497.97	27 870.1	13 123.0	35 549.5	19 900.2	46 479.3
	2	19 005.5	51 831.5	25 255.7	62 786.5	35 544.8	77 232.5
	3	30 762.2	78 943.5	39 460.8	92 333.4	52 440.9	80 291.1
1	0	3163.43	9542.25	4535.80	13 067.2	7771.92	19 146.4
	1	9955.27	28 052.7	13 803.0	35 779.9	21 383.6	46 803.1
	2	19 609.7	52 004.1	26 152.4	62 993.7	37 152.3	77 431.4
	3	31 454.1	79 099.2	40 452.5	92 510.6	53 914.7	80 800.4
2	0	4390.84	10 058.8	6364.60	13 754.3	11 172.5	20 253.7
	1	11 789.5	28 608.5	16 456.4	36 481.8	25 749.1	47 777.1
	2	21 779.3	52 524.6	29 178.7	63 617.7	41 607.0	78 077.3
	3	33 781.5	79 567.2	43 572.6	93 042.4	58 073.4	82 031.6
S–C annular plates							
0	0	3750.49	10 075.5	5402.73	13 863.2	9085.09	20 467.1
	1	10 405.7	28 498.0	14 405.2	36 349.0	21 620.1	47 153.5
	2	19 981.0	52 398.6	26 550.3	63 395.2	36 779.0	77 783.1
	3	31 750.0	79 414.0	40 642.6	92 743.8	53 159.8	82 956.4
1	0	4058.98	10 269.4	5786.68	14 097.9	9650.30	20 712.9
	1	11 011.7	28 696.1	15 165.1	36 577.6	22 760.9	47 428.9
	2	20 698.9	52 572.8	27 410.6	63 586.2	37 967.1	77 862.7
	3	32 495.3	79 564.8	41 504.8	92 903.7	54 329.9	83 992.4
2	0	5721.77	10 881.2	8154.09	14 854.8	13 399.6	21 608.9
	1	13 372.0	29 296.8	18 295.4	37 274.2	27 071.5	48 275.8
	2	23 306.8	53 097.5	30 658.5	64 164.0	42 085.2	78 291.4
	3	35 101.6	80 018.5	44 597.2	93 386.1	58 067.0	85 611.8

higher degrees of the edge constraint (in order from soft simply-supported to hard simply-supported to clamped) are applied to the plate edges.

5.2. Effect of piezoelectric layer

Fig. 2 shows the behavior of the natural frequencies ω (rad/s) as a function of thickness of piezoelectric layers for an annular plate under C–S* boundary condition when r_1=0.3 m, r_0=1 m and h=0.05 m. According to Fig. 2, the higher natural frequencies (i.e., modes (0, 1), (1, 1) and (2, 1)) initially decreases when the h_p/h varies between 0 and 0.05, and then increases when $h_p/h>0.05$. However, with the increase of the piezoelectric thickness, the lower natural frequencies (i.e., modes (0,0), (1,0) and (2,0)) continuously increases. Fig. 3 contains the plot of the fundamental frequency ω_1 (rad/s) versus h_p/h for the S–S annular Levinson plate (r_1=0.5 m, r_0=1 m and h=0.05 m) for three different common piezoelectric materials (PZT (NECPEC6), PZT4 and PIC-151). It can be deduced from Fig. 3 that with the increase of the piezoelectric thickness, the fundamental frequency for PZT and PZT4 increases monotonously, whereas for PIC-151 the fundamental frequency initially diminishes and then increases with the enhancement of the h_p/h. Duan et al. [21] reported that increasing of piezoelectric thickness can increase or decrease the frequencies. Using thicker piezoelectric layers increases bending stiffness of the plate that causes to enhance the frequencies, however the effect of piezoelectricity diminishes frequencies. The behavior of PIC-151 in Fig. 3 arises from the fact that when thinner piezoelectric layers are used, the effect of piezoelectricity is more dominant than that of plate stiffness. Another interesting point about Fig. 3 is that the increase in frequency is smaller for PIC-151 than two others materials.

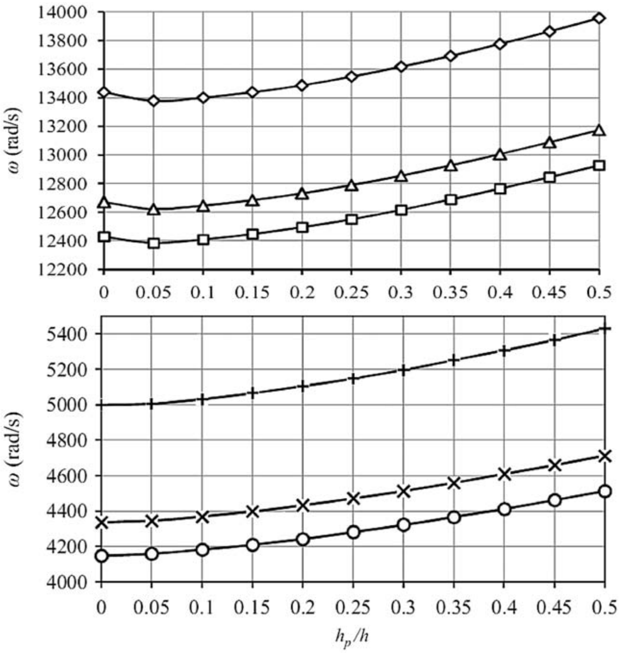

Fig. 2. Variation of the frequencies ω (rad/s) for an annular plate under C–S* boundary condition against the thickness of piezoelectric layers for different modes when $r_1 = 0.3$ m, $r_0 = 1$ m and $h = 0.05$ m. —◇— mode(2,1); —△— mode(1,1); —□— mode(0,1); —+— mode(2,0); —×— mode(1,0); —○— mode(0,0).

5.3. Three-dimensional mode shapes

To have a more appropriate sense of the transverse displacement w, three first mode shapes of an annular Levinson coupled piezoelectric plate, $h/r_0 = 0.1$, $r_1 = 0.5$, $r_0 = 1$ and $h_p/h = 0.05$ are illustrated in Fig. 4 for C–C and C–S boundary conditions, respectively.

6. Concluding remarks

In this paper, the free vibration of a three-layer piezoelectric laminated annular plate based on the Levinson plate theory is investigated for the case where the electrodes on the piezoelectric layers are shortly connected. The electric potential distribution across thickness of piezoelectric layer is modeled by a sinusoidal function and Maxwell equation is enforced. Analytical solutions are presented and the closed-form characteristic equations, displacement field of the plate and the electric potential are derived for the first time. Comparison studies proved that the present method is in good agreement with other methods reported in the literature for different boundary conditions of the plate. Parametric studies were devoted to the effects of the thickness-radius ratio, inner–outer radius ratio, thickness of piezoelectric and material of piezoelectric on the natural frequencies of the piezoelectric coupled annular plate. Finally, some 3-D plots were shown for the mode shapes of the annular Levinson plates. Due to the inherent features of the present solution, all findings will be a useful benchmark for evaluating other analytical and numerical methods developed by researchers in the future.

Appendix A

Some coefficients referred to in this paper are given as follows:

$$(A,B,C,D,F,G) = \int_{-h}^{h} E(1,z,z^2,z^3,z^4,z^6)\,\mathrm{d}z, \tag{A.1}$$

$$t_1 = \tfrac{2}{3}\,[(h+h_p)^3 - h^3], \quad t_2 = \tfrac{2}{5}[(h+h_p)^5 - h^5], \tag{A.2,3}$$

$$D_1 = \frac{C}{1-\nu^2} - \frac{F}{3(h+h_p)^2(1-\nu^2)}, \quad D_2 = \overline{C}_{11} t_1 - \frac{\overline{C}_{11} t_2}{3(h+h_p)^2}, \tag{A.3,4}$$

$$S_1 = \frac{F\nu}{3(h+h_p)^2(1-\nu^2)} + \frac{\overline{C}_{12} t_2}{3(h+h_p)^2}, \quad S_2 = \frac{F(\nu-1)}{3(h+h_p)^2(1-\nu^2)} + \frac{t_2(\overline{C}_{12} - \overline{C}_{11})}{3(h+h_p)^2},$$

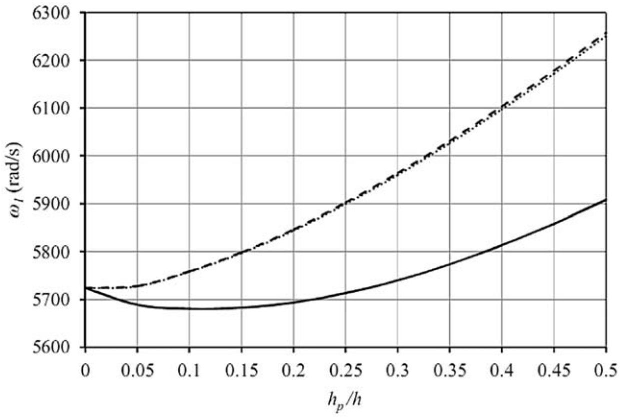

Fig. 3. The fundamental frequency ω_1 (rad/s) for an annular plate under S–S boundary condition with different piezoelectric materials versus the thickness of piezoelectric layer for $r_1 = 0.5$ m, $r_0 = 1$ m and $h = 0.05$ m. ▬ ▬ ▬ PZT (NECPEC6); ▪▪▪▪▪▪▪▪ PZT4; ▬▬▬▬ PIC-151.

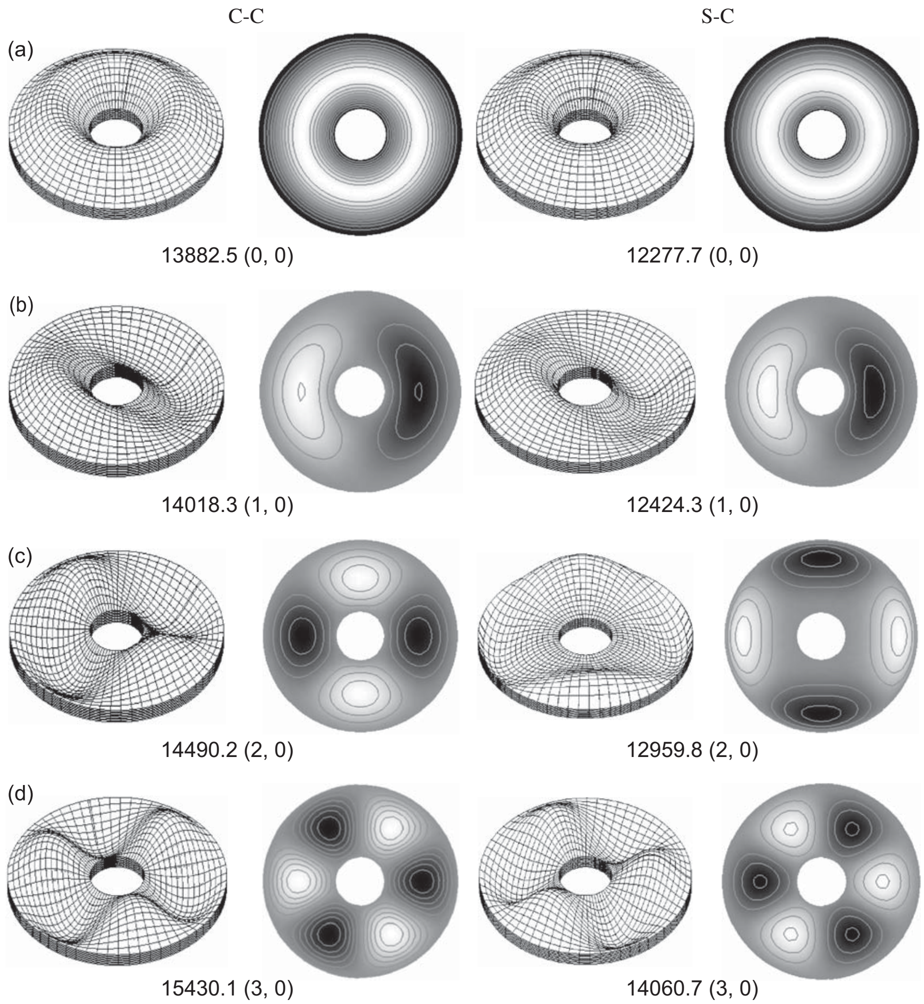

Fig. 4. Deformed mode shapes and frequencies (rad/s) of annular plate under C–C and C–S boundary conditions ($h/r_0 = 0.1$, $r_1 = 0.5$, $r_0 = 1$ and $h_p/h = 0.05$).

$$S_3 = \frac{F}{3(h+h_p)^2(1-\nu^2)} + \frac{\overline{C}_{11}t_2}{3(h+h_p)^2}, \tag{A.4−7}$$

$$A_1 = \frac{1}{2}\left[(1-\nu)D_1 + \left(1-\frac{\overline{C}_{12}}{\overline{C}_{11}}\right)D_2\right],$$

$$A_2 = \left(\frac{A}{2(1+\nu)} - \frac{C}{2(h+h_p)^2(1+\nu)} + 2C_{55}h_p - \frac{C_{55}t_1}{(h+h_p)^2}\right), \quad A_3 = \frac{4h_p}{\pi}(e_{15}-\overline{e}_{31})$$

$$A_4 = 1 - \frac{\overline{e}_{31}h_p}{(e_{15}+\overline{e}_{31})\left(h_p - \frac{t_1}{2(h+h_p)^2}\right)}, \quad A_5 = \frac{2\Xi_{11}h_p}{\pi(e_{15}+\overline{e}_{31})\left(h_p - \frac{t_1}{2(h+h_p)^2}\right)},$$

$$A_6 = \frac{2\overline{\Xi}_{33}\pi}{h_p(e_{15}+\overline{e}_{31})\left(h_p - \frac{t_1}{2(h+h_p)^2}\right)}, \quad A_7 = \frac{I_5}{3(h+h_p)^2}, \quad A_8 = \frac{4}{\pi}h_p e_{15}, \tag{A.8−15}$$

$$P_1 = \frac{-A_2A_5(D_1+D_2+S_3) + A_8(A_4(D_1+D_2)+S_3)}{A_6(A_3-A_8)}, \tag{A.16}$$

$$P_2 = \frac{A_5A_7S_3}{A_3A_6 - A_6A_8}, \tag{A.17}$$

$$P_3 = \frac{A_2(A_3(A_4-1) + A_8 - A_4A_8 + A_6(D_1+D_2+S_3))}{A_6(A_3-A_8)}, \tag{A.18}$$

$$P_4 = \frac{-A_3A_4A_7 + A_5(D_1+D_2)I_1 - A_4A_8\bar{I}_3 + A_2A_5(2A_7+\bar{I}_3) - A_7(A_8+A_6S_3)}{A_6(A_3-A_8)}, \tag{A.19}$$

$$P_5 = \frac{A_5A_7^2}{A_6(A_8-A_3)}, \tag{A.20}$$

$$P_6 = \frac{A_6A_7^2 - A_5I_1\bar{I}_3}{A_3A_6 - A_6A_8}, \tag{A.21}$$

$$P_7 = \frac{(A_3 - A_6(D_1+D_2))I_1 - A_2(A_5I_1 + A_6(2A_7+\bar{I}_3))}{A_6(A_3-A_8)}, \tag{A.22}$$

$$P_8 = \frac{I_1\bar{I}_3}{A_3-A_8}, \tag{A.23}$$

$$P_9 = \frac{I_1A_2}{A_3-A_8}, \tag{A.24}$$

$$K_1 = \frac{1}{(A_2A_5 - A_8 + A_5A_7\omega^2)^2}(A_6(A_2^2A_5(A_3-A_8) + \omega^2(A_3A_7(A_5A_7\omega^2 - A_8) + A_8(A_6A_7(D_1+D_2) - A_8\bar{I}_3 + A_5A_7\bar{I}_3\omega^2)) \\ + A_2(-A_3(A_8 - 2A_5A_7\omega^2) + A_8(A_8 + A_6(D_1+D_2) + A_5(\bar{I}_3 - A_7)\omega^2)))), \tag{A.25}$$

$$K_2 = S_3 + \frac{(A_2A_5 - A_4A_8)(D_1+D_2)}{A_2A_5 - A_8 + A_5A_7\omega^2}, \tag{A.26}$$

$$K_3 = A_2 - A_2A_4 + A_7\omega^2 + A_4\bar{I}_3\omega^2 + \frac{(A_2(A_4-1) + A_4A_7\omega^2)(-A_3 + A_2A_5 + A_6(D_1+D_2) - A_5\bar{I}_3\omega^2)}{A_2A_5 - A_8 + A_5A_7\omega^2} \\ + \frac{1}{(A_2A_5 - A_8 + A_5A_7\omega^2)^2}(A_5(D_1+D_2)(-A_2^2(A_4-1)A_6 + (-A_8I_1 + A_2((1-2A_4)A_6A_7 + A_5I_1))\omega^2 \\ + A_7(-A_4A_6A_7 + A_5I_1)\omega^4)), \tag{A.27}$$

$$K_4 = \frac{1}{(A_2A_5 - A_8 + A_5A_7\omega^2)^2}(I_1\omega^2(-A_2^2A_5^2 + A_6A_8(D_1+D_2) + A_3(A_5A_7\omega^2 - A_8) + A_5\bar{I}_3\omega^2(A_5A_7\omega^2 - A_8) + A_2A_5(A_3 + A_8 + A_5(\bar{I}_3 - A_7)\omega^2))). \tag{A.28}$$

Appendix B

There exists closed-form solutions to the characteristic equations of annular plate under all possible combinations of soft simply supported, hard simply supported and clamped boundary conditions.

Substituting Eqs. (10), (37), (45) and (50) into boundary conditions, given by Eqs. (51)–(53), yields an eighth-order determinant for the frequency parameters ω. For the sake of clarity, the determinant will not be expanded and the characteristic equations are represented in a matrix form. First four rows of the 8×8 matrix are related to the boundary conditions at the inner edge, while second ones are related to those at the outer edge. Thus, the 8×8 matrix is divided into two 4×8 sub-matrices corresponding to boundary conditions at the inner and outer edges of the plate. Following sub-matrices are given for clamped, hard simply supported and soft simply supported boundary conditions:

Case 1. Clamped annular plates

$$A=\begin{vmatrix} w_{11}(\chi_1 r) & w_{12}(\chi_1 r) & w_{21}(\chi_2 r) & w_{22}(\chi_2 r) & w_{31}(\chi_3 r) & w_{32}(\chi_3 r) & 0 & 0 \\ a_1 w'_{11}(\chi_1 r) & a_1 w'_{12}(\chi_1 r) & a_2 w'_{21}(\chi_2 r) & a_2 w'_{22}(\chi_2 r) & a_3 w'_{31}(\chi_3 r) & a_3 w'_{32}(\chi_3 r) & \dfrac{p w_{41}(\chi_4 r)}{r} & \dfrac{p w_{42}(\chi_4 r)}{r} \\ \dfrac{p}{r} a_1 w_{11}(\chi_1 r) & \dfrac{p}{r} a_1 w_{12}(\chi_1 r) & \dfrac{p}{r} a_2 w_{21}(\chi_2 r) & \dfrac{p}{r} a_2 w_{22}(\chi_2 r) & \dfrac{p}{r} a_3 w_{31}(\chi_3 r) & \dfrac{p}{r} a_3 w_{32}(\chi_3 r) & w'_{41}(\chi_4 r) & w'_{42}(\chi_4 r) \\ \Gamma_1(r) & \Gamma\Gamma_1(r) & \Gamma_2(r) & \Gamma\Gamma_2(r) & \Gamma_3(r) & \Gamma\Gamma_3(r) & \Gamma_4(r) & \Gamma\Gamma_4(r) \end{vmatrix}, \tag{B.1}$$

where the prime ($'$) indicates the derivative with respect to the r; $w_{ij}(p,\chi_i r)$ is concisely expressed as $w_{ij}(\chi_i r)$; $\cos(p\theta)e^{i\omega t}$ and $\sin(p\theta)e^{i\omega t}$ are eliminated for the brevity and we have

$$\Gamma_i(r)=\left(e_{15}\left(\frac{\pi h_p(3h+2h_p)}{3(h+h_p)^2}\right)(1+a_i)-2\Xi_{11}L_i\right)w'_{i1}(\chi_i r),\quad i=1,2,3, \tag{B.2}$$

$$\Gamma_4(r)=e_{15}\left(\frac{\pi h_p(3h+2h_p)}{3(h+h_p)^2}\right)\frac{p}{r}w_{41}(\chi_4 r), \tag{B.3}$$

$$\Gamma\Gamma_i(r)=\left(e_{15}\left(\frac{\pi h_p(3h+2h_p)}{3(h+h_p)^2}\right)(1+a_i)-2\Xi_{11}L_i\right)w'_{i2}(\chi_i r),\quad i=1,2,3, \tag{B.4}$$

$$\Gamma\Gamma_4(r)=e_{15}\left(\frac{\pi h_p(3h+2h_p)}{3(h+h_p)^2}\right)\frac{p}{r}w_{42}(\chi_4 r). \tag{B.5}$$

Case 2. Hard simply supported annular plates

$$B=\begin{vmatrix} w_{11}(\chi_1 r) & w_{12}(\chi_1 r) & w_{21}(\chi_2 r) & w_{22}(\chi_2 r) & w_{31}(\chi_3 r) & w_{32}(\chi_3 r) & 0 & 0 \\ \mu_1(r) & \mu\mu_1(r) & \mu_2(r) & \mu\mu_2(r) & \mu_3(r) & \mu\mu_3(r) & \mu_4(r) & \mu\mu_4(r) \\ \dfrac{p}{r} a_1 w_{11}(\chi_1 r) & \dfrac{p}{r} a_1 w_{12}(\chi_1 r) & \dfrac{p}{r} a_2 w_{21}(\chi_2 r) & \dfrac{p}{r} a_2 w_{22}(\chi_2 r) & \dfrac{p}{r} a_3 w_{31}(\chi_3 r) & \dfrac{p}{r} a_3 w_{32}(\chi_3 r) & w'_{41}(\chi_4 r) & w'_{42}(\chi_4 r) \\ \Gamma_1(r) & \Gamma\Gamma_1(r) & \Gamma_2(r) & \Gamma\Gamma_2(r) & \Gamma_3(r) & \Gamma\Gamma_3(r) & \Gamma_4(r) & \Gamma\Gamma_4(r) \end{vmatrix}, \tag{B.6}$$

where

$$\mu_i(r)=((D_1+D_2)a_i-S_1+S_2)w''_{i1}(\chi_i r)+\left((D_1+D_2-2A_1)\frac{a_i}{r}-\frac{S_1}{r}\right)w'_{i1}(\chi_i r)-\left(\frac{p^2}{r^2}(D_1+D_2-2A_1)a_i+\frac{4}{\pi}h_p\overline{e}_{31}L_i-\frac{p^2}{r^2}S_1\right)w_{i1}(\chi_i r),\quad i=1,2,3, \tag{B.7}$$

$$\mu_4(r)=\frac{2A_1 p}{r}\left(w'_{41}(r)-\frac{w_{41}(r)}{r}\right), \tag{B.8}$$

$$\begin{aligned}\mu\mu_i(r)=&((D_1+D_2)a_i-S_1+S_2)w''_{i2}(\chi_i r)+\left((D_1+D_2-2A_1)\frac{a_i}{r}-\frac{S_1}{r}\right)w'_{i2}(\chi_i r)\\&-\left(\frac{p^2}{r^2}(D_1+D_2-2A_1)a_i+\frac{4}{\pi}h_p\overline{e}_{31}L_i-\frac{p^2}{r^2}S_1\right)w_{i2}(\chi_i r),\quad i=1,2,3,\end{aligned} \tag{B.9}$$

$$\mu\mu_4(r)=\frac{2A_1 p}{r}\left(w'_{42}(r)-\frac{w_{42}(r)}{r}\right), \tag{B.10}$$

Table B1
Closed-form characteristic equations for annular plates with different combination of boundary conditions in matrix forms.

Boundary conditions at inner edge	Boundary conditions at outer edge		
	Soft simply supported	Hard simply supported	Clamped
Clamped	$\begin{bmatrix} A\|_{r=r_1} \\ C\|_{r=r_0} \end{bmatrix}_{8\times 8}$	$\begin{bmatrix} A\|_{r=r_1} \\ B\|_{r=r_0} \end{bmatrix}_{8\times 8}$	$\begin{bmatrix} A\|_{r=r_1} \\ A\|_{r=r_0} \end{bmatrix}_{8\times 8}$
Hard simply supported	$\begin{bmatrix} B\|_{r=r_1} \\ C\|_{r=r_0} \end{bmatrix}_{8\times 8}$	$\begin{bmatrix} B\|_{r=r_1} \\ B\|_{r=r_0} \end{bmatrix}_{8\times 8}$	$\begin{bmatrix} B\|_{r=r_1} \\ A\|_{r=r_0} \end{bmatrix}_{8\times 8}$
Hard simply supported	$\begin{bmatrix} C\|_{r=r_1} \\ C\|_{r=r_0} \end{bmatrix}_{8\times 8}$	$\begin{bmatrix} C\|_{r=r_1} \\ B\|_{r=r_0} \end{bmatrix}_{8\times 8}$	$\begin{bmatrix} C\|_{r=r_1} \\ A\|_{r=r_0} \end{bmatrix}_{8\times 8}$

Case 3. Soft simply supported annular plates

$$C=\begin{vmatrix} w_{11}(\chi_1 r) & w_{12}(\chi_1 r) & w_{21}(\chi_2 r) & w_{22}(\chi_2 r) & w_{31}(\chi_3 r) & w_{32}(\chi_3 r) & 0 & 0 \\ \mu_1(r) & \mu\mu_1(r) & \mu_2(r) & \mu\mu_2(r) & \mu_3(r) & \mu\mu_3(r) & \mu_4(r) & \mu\mu_4(r) \\ \alpha_1(r) & \alpha\alpha_1(r) & \alpha_2(r) & \alpha\alpha_2(r) & \alpha_3(r) & \alpha\alpha_3(r) & \alpha_4(r) & \alpha\alpha_4(r) \\ \Gamma_1(r) & \Gamma\Gamma_1(r) & \Gamma_2(r) & \Gamma\Gamma_2(r) & \Gamma_3(r) & \Gamma\Gamma_3(r) & \Gamma_4(r) & \Gamma\Gamma_4(r) \end{vmatrix}, \tag{B.11}$$

where

$$\alpha_i(r)=(2A_1a_i+S_2)\left(\frac{p}{r}w'_{i1}\ (\chi_i r)-\frac{p}{r^2}w_{i1}(\chi_i r)\right),\quad i=1,2,3, \tag{B.12}$$

$$\alpha_4(r)=A_1\left(\frac{p^2}{r^2}w_{41}(\chi_4 r)+w''_{41}\ (\chi_4 r)-\frac{w'_{41}\ (\chi_4 r)}{r}\right), \tag{B.13}$$

$$\alpha\alpha_i(r)=(2A_1a_i+S_2)\left(\frac{p}{r}w'_{i2}\ (\chi_i r)-\frac{p}{r^2}w_{i2}(\chi_i r)\right),\quad i=1,2,3, \tag{B.14}$$

$$\alpha\alpha_4(r)=A_1\left(\frac{p^2}{r^2}w_{42}(\chi_4 r)+w''_{42}\ (\chi_4 r)-\frac{w'_{42}\ (\chi_4 r)}{r}\right). \tag{B.15}$$

For each case, a closed-form solution can be obtained by setting the determinant of the matrices in Table B1 equal to zero. Roots of the determinant are the natural frequencies of annular plates with specific boundary conditions at inner and outer edges of annular plates for a given wave number.

References

[1] A.W. Leissa, *Vibration of Plates (NASA SP-160)*, Office of Technology Utilization, Washington, DC, 1969.
[2] T. Irie, G. Yamada, K. Takagi, Natural frequencies of thick annular plates, *Journal of Applied Mechanics* 49 (3) (1982) 633–638.
[3] J. So, A.W. Leissa, Three-dimensional vibrations of thick circular and annular plates, *Journal of Sound and Vibration* 209 (1998) 15–41.
[4] K.M. Liew, B. Yang, Elasticity solutions for free vibrations of annular plates from three-dimensional analysis, *International Journal of Solids and Structures* 37 (2000) 7689–7702.
[5] E. Efraim, M. Eisenberger, Exact vibration analysis of variable thickness thick annular isotropic and FGM plates, *Journal of Sound and Vibration* 299 (2007) 720–738.
[6] C.F. Liu, Y.T. Lee, Finite element analysis of three-dimensional vibrations of thick circular and annular plates, *Journal of Sound and Vibration* 233 (1) (2000) 63–80.
[7] D. Zhou, F.T.K. Au, Y.K. Cheung, S.H. Lo, Three-dimensional vibration analysis of circular and annular plates via the Chebyshev–Ritz method, *International Journal of Solids and Structures* 40 (2003) 3089–3105.
[8] E. Reissner, The effect of transverse shear deformation on the bending of elastic plates, *Journal of Applied Mechanics* 12 (1945) 69–77.
[9] R.D. Mindlin, Influence of rotary inertia and shear in flexural motion of isotropic elastic plates, *Journal of Applied Mechanics* 18 (1951) 31–38.
[10] R.D. Mindlin, H. Deresiewicz, Thickness-shear and flexural vibrations of a circular disk, *Journal of Applied Physics* 25 (1954) 1329–1332.
[11] J.N. Reddy, A general third-order nonlinear theory of plates with moderate thickness, *International Journal of Non-linear Mechanics* 25 (1990) 677–686.
[12] M. Levinson, An accurate, simple theory of the static's and dynamics of elastic plates, *Mechanics Research Communications* 7 (6) (1980) 343–350.
[13] C.M. Wang, S. Kitipornchai, Frequency relationship between Levinson plates and classical thin plates, *Mechanics Research Communications* 26 (6) (1999) 687–692.
[14] J.N. Reddy, C.M. Wang, G.T. Lim, K.H. Ng, Bending solutions of Levinson beams and plates in terms of the classical theories, *International Journal of Solids and Structures* 38 (2001) 4701–4720.
[15] A. Nosier, J.N. Reddy, Part I: on vibration and buckling of symmetric laminated plates according to shear deformations theories, *Acta Mechanica* 94 (1992) 123–144.
[16] A. Nosier, J.N. Reddy, Part II: on vibration and buckling of symmetric laminated plates according to shear deformations theories, *Acta Mechanica* 94 (1992) 145–169.
[17] H.F. Tiersten, *Linear Piezoelectric Plate Vibration*, Plenum, New York, 1969 (Chapter 5).
[18] H. Ding, R. Xu, Y. Chi, W. Chen, Free axisymmetric vibration of transversely isotropic piezoelectric circular plates, *International Journals of Solids and Structures* 36 (1999) 4629–4652.
[19] Q. Wang, S.T. Quek, C.T. Sun, X. Liu, Analysis of piezoelectric coupled circular plate, *Smart Materials and Structures* 10 (2001) 229–239.

[20] X. Liu, Q. Wang, S.T. Quek, Analytical solution for free vibration of piezoelectric coupled moderately thick circular plates, *International Journal of Solids and Structures* 39 (2002) 2129–2151.
[21] W.H. Duan, S.T. Quek, Q. Wang, Free vibration analysis of piezoelectric coupled thin and thick annular plate, *Journal of Sound and Vibration* 281 (2005) 119–139.
[22] C.F. Liu, T.J. Chen, Y.J. Chen, A modified axisymmetric finite element for the 3-D vibration analysis of piezoelectric laminated circular and annular plates, *Journal of Sound and Vibration* 309 (2008) 794–804.
[23] X.D. Zhang, C.T. Sun, Analysis of sandwich plate containing a piezoelectric core, *Smart Materials and Structures* 8 (1999) 31–40.
[24] M.R. Speigel, *Mathematical Handbook of Formulas and Tables, Schaum's Outline Series*, McGraw-Hill, Singapore, 1999.